

Ergodicity in a two-dimensional self gravitating many body system

C. H. Silvestre

Instituto de Física – Universidade de Brasília

CP: 04455, 70919-970 - Brasília, Brazil

T. M. Rocha Filho

Instituto de Física and International Center for Condensed Matter Physics

Universidade de Brasília, CP: 04455, 70919-970 - Brasília, Brazil

Abstract

We study the ergodic properties of a two-dimensional self-gravitating system using molecular dynamics simulations and applying three tests for ergodicity: a direct method comparing the time average of a particle momentum to ensemble averages, sojourn times statistics for cells in momentum space and the dynamical functional method. These methods are also applied to a short-range interacting system for comparison purposes. Our results show a two-dimensional self-gravitating system takes a very long time to establish ergodicity which is independent on particle number, at variance with what is observed in a few simplified models of long-range interacting systems.

I. INTRODUCTION

N -body systems with long range interactions presents some peculiarities with respect to systems with short-range interactions, having drawn much attention at least along the last two decades [1–5] and even more if one considers self-gravitating systems and charged plasmas. Starting from a non-equilibrium configuration, a short-interacting system evolves to thermodynamic equilibrium in a relatively small relaxation time, while a long-range interacting system evolves over different stages characterized by time-scales differing by orders of magnitude, taking a very long time to reach thermodynamic equilibrium for a finite number of particles, and never attains it in the $N \rightarrow \infty$ Vlasov limit. The initial stage of evolution is a violent relaxation into a Quasi-Stationary State (QSS) in a time roughly independent on the number of particles [6], and then relaxes very slowly to equilibrium for finite N . A pair interaction potential is long-ranged if it decays at long distances as $r^{-\alpha}$ with $\alpha < d$, d the spatial dimension and r the inter-particle distance. This implies that all particles, no matter how far, contribute to the total energy. Consequently the system is non-additive, violating one of the fundamental axioms of thermodynamics: entropy is non-additive even at equilibrium. It is worth remembering that this is not in contradiction to the second law of Thermodynamics, which is always valid. Another common consequence is non-ergodicity, most extensively studied for the Hamiltonian mean field model [7–14], but also for one and three-dimensional self gravitating systems [16–18].

The study of ergodicity was pioneered by Boltzmann in his works on the foundations on Statistical Mechanics [19] and latter extended by Birkhoff [20] and Khinchin [21]. The ergodic hypothesis states that for large systems of interacting particles time averages equals the ensemble or equilibrium averages:

$$\lim_{t_f \rightarrow \infty} \frac{1}{t_f - t_0} \int_{t_0}^{t_f} dt b(x_t) \equiv \bar{b}(x) = \langle b(x) \rangle \equiv \int d\mu_0 b(x), \quad (1)$$

where x denotes a point in phase-space, $b(x)$ is a dynamical function, $\bar{b}(x)$ its time average, $\langle b(x) \rangle$ its ensemble average and $d\mu_0$ a statistical measure. This is equivalent to state that the total time spent in a phase-space region is asymptotically proportional to its measure. Proving ergodicity rigorously is a difficult task and has been accomplished only for a few cases, and most studies rely on different methods to ascertain ergodicity such as determining the existence of gaps in phase-space [8, 10], direct comparison of time and ensemble averages

for the velocity variable [9], sojourn time statistics for cells in phase-space [15, 22, 23], testing for equipartition of energy [16, 17, 24] and the dynamical functional approach [25–27]. The latter can also be used to determine whether the system is mixing, which is a stronger property than ergodicity. Non-ergodicity can also be classified as strong if some regions of phase-space are non-accessible to the system and weak if all regions are accessible but not equally visited.

In this paper we study the ergodic properties of a two-dimensional self-gravitating N -body system by comparing it to a short-range interacting system. For that purpose we use the direct, sojourn times and the dynamical functional methods. A two dimensional self-gravitating system with N identical particles is described by the Hamiltonian:

$$H = \sum_{k=1}^N \frac{p_k^2}{2} + \frac{1}{2N} \sum_{k,l=1}^N \ln(|\mathbf{r}_k - \mathbf{r}_l| + \epsilon), \quad (2)$$

where the logarithmic potential is the solution of the Poisson equation in two-dimensions [29], all masses are set to unity and ϵ is a softening small parameter, commonly used in simulations of self-gravitating systems to avoid the divergence in the potential at zero distance [36]. The potential in Eq. (2) is not upper bound and therefore is confining, thus avoiding the difficulty of particle evaporation in three-dimensional gravity. This model was used for instance in the study of anomalous diffusion in a collapsing phase [30], the determination of thermodynamic equilibrium [31], collisional relaxation [32, 33], violent relaxation [29, 34] and cooling in self-gravitating accretion discs [35].

For comparison purposes it is useful to study a similar system but with short-range interactions. We introduce then the two-dimensional system described by the Hamiltonian

$$H = \sum_{k=1}^N \frac{p_k^2}{2} + \frac{1}{2N} \sum_{k,l=1}^N \frac{1}{(|\mathbf{r}_k - \mathbf{r}_l| + \epsilon)^\alpha}, \quad (3)$$

with $\alpha > 2$ ensuring that the interaction is short-ranged, and the Kac factor $1/N$ is kept in order to have similar time scales for both systems. As the potential is no longer confining, periodic boundary conditions are used.

The structure of the paper is as follows: In section II we succinctly present the three methods cited above for testing ergodicity. Section III is devoted to apply such methods for the short-range interacting system with Hamiltonian in Eq. (3), while the ergodic properties of the two-dimensional self-gravitating system are studied in Section IV. We close the paper with some concluding remarks in Section V.

II. TESTING ERGODICITY

A. Direct method

For a mean-field system we can consider a single particle evolution and compute the ensemble average by taking the average over the N particles in the whole system. For an ergodic system both quantities coincide. Let us then consider the momentum $p_k(t)$ of particle k at time t and write its time average as:

$$\bar{p}_k = \frac{1}{m} \sum_{j=0}^m p_k(j\Delta t), \quad (4)$$

where Δt will correspond to the numeric integration time step and m is the number of time intervals. The ensemble average at time t is given by

$$\langle p(t) \rangle = \frac{1}{N} \sum_{i=0}^N p_i(t). \quad (5)$$

For an ergodic system \bar{p}_k is the same for all particles, and therefore its standard deviation:

$$\sigma(t) = \sqrt{\frac{1}{N} \sum_{k=1}^N \bar{p}_k^2(t)}, \quad (6)$$

would tend to zero (we assumed $\langle \bar{p}_k \rangle = 0$). The direct method then consists in verifying numerically if $\sigma(t)$ vanishes (or approaches zero) for some time t . This approach was used in Ref. [9] for the Hamiltonian mean field model.

B. Sojourn time statistics

This approach is due to Rebenshtok and Barkai in the context of a Continuous Time Random Walk (CTRW) [22]. Consider a system of discrete states labeled by an integer index, each one visited intermittently for a given time. The time spent in the state k during the j -th visitation is denoted by $t_{k,j}^{(s)}$ and called a sojourn time. The sum over all sojourn times for a given state yields its residence time:

$$t_k = \sum_j t_{k,j}^{(s)}. \quad (7)$$

The probability density function for a weak non-ergodic system for the time average $\bar{\mathcal{O}}$ of an observable \mathcal{O} can be written as [22]:

$$f^{(\alpha)}(\bar{\mathcal{O}}) = \frac{1}{\pi} \lim_{\epsilon \rightarrow 0} \text{Im} \left[\frac{\sum_{k=1}^L p_k^{eq} (\bar{\mathcal{O}} - \bar{\mathcal{O}}_k + i\epsilon)^{\alpha/2-1}}{\sum_{k=1}^L p_k^{eq} (\bar{\mathcal{O}} - \bar{\mathcal{O}}_k + i\epsilon)^{\alpha/2}} \right], \quad (8)$$

where α is a constant in the interval $(0, 2]$, \mathcal{O}_k is the value of the observable in state k , p_k^{eq} is the probability for the system to be in the state k and L the number of discrete states. The time average of the observable \mathcal{O} is thus:

$$\overline{\mathcal{O}} = \frac{1}{t_{tot}} \sum_{k=1}^L t_k \mathcal{O}_k, \quad (9)$$

with $t_{tot} = \sum_{i=1}^L t_i$. Rebenshtok and Barkai then showed that if the statistics of the sojourn times $t_{k,j}^{(s)}$ have a power law tail, then the system is non-ergodic. In the limit $\alpha \rightarrow 2$ one obtains $f^{(\alpha)}(\overline{\mathcal{O}}) \rightarrow \delta(\overline{\mathcal{O}} - \langle \mathcal{O} \rangle)$ and thus

$$f^2(\overline{\mathcal{O}}) = \delta(\overline{\mathcal{O}} - \langle \overline{\mathcal{O}} \rangle), \quad (10)$$

meaning that the system is ergodic. Usually for a finite system the time a particle spends in a given cell cannot be arbitrarily large, and the distribution of sojourn times must be truncated at some value of time. For the Hamiltonian mean field model the statistics of sojourn times exhibits a truncated algebraic tail with a truncation time diverging with N , indicating that the time for ergodicity is very large and diverges with N , such that the system is non-ergodic only in the limit $N \rightarrow \infty$ [15].

C. Dynamical functional method

For a stationary infinitely divisible processes $Y(n)$, with n integer, the dynamical functional is given by the Fourier transform with unit wave number of the process $Y(n) - Y(0)$ [25–27]:

$$D(n) = \left\langle e^{i[Y(n) - Y(0)]} \right\rangle, \quad (11)$$

where $\langle \dots \rangle$ denotes the ensemble average, i. e. an average over many realizations of the stochastic process $Y(n)$. For our purposes in the present work the stochastic process is given by the values the momentum of a given particle $Y(n) = p_k(n\Delta t)$, while the ensemble average is taken over the N particles of the system. The system is ergodic if and only if [27]:

$$\lim_{n \rightarrow \infty} \frac{1}{n} \sum_{k=1}^{n-1} D(k) = |\langle e^{ip(0)} \rangle|^2, \quad (12)$$

and mixing if and only if:

$$\lim_{n \rightarrow \infty} D(n) = |\langle e^{ip(0)} \rangle|^2. \quad (13)$$

It is useful to define the new functions:

$$\begin{aligned} E(n) &\equiv D(n) - |\langle e^{ip(0)} \rangle|^2, \\ Q(n) &\equiv \frac{1}{n} \sum_{k=1}^{n-1} E(k). \end{aligned} \tag{14}$$

Then Eqs. (12) and (13) are rewritten, respectively, as:

$$\lim_{n \rightarrow \infty} Q(n) = 0, \tag{15}$$

and

$$\lim_{n \rightarrow \infty} E(n) = 0. \tag{16}$$

Testing for mixing is of special interest as many theories for violent relaxation presuppose a good mixing in the initial evolution [6] (see also [37] and references therein).

The time required for the system to reach ergodicity, i. e. the time at which the difference in the time and ensemble averages is negligible will be called from here on time for ergodicity.

III. SHORT-RANGE INTERACTING SYSTEM

As an illustration of the methods described in the previous section, let us consider the Hamiltonian with short-range interactions in Eq. (3) with $\alpha = 3$. All simulations in the present paper were performed using a parallel implementation on a Graphics Processing Unit (GPU) [28]. The system first evolves for a sufficient time to reach thermodynamic equilibrium. To apply the direct method we compute the time average of the momentum of each particle and then compute the standard deviation $\sigma(t)$ of these averages over the ensemble of N particles, as given by Eq. (6). Results for $N = 512$ and $N = 2048$ are shown in Fig. 1. The least-squares fit for the algebraic tail of the function $\sigma(t)$ is also shown and has an exponent -0.493 , very close to the value for a sum of uncorrelated random variables as predicted from the central limit theorem. We observe that the standard deviation rapidly approaches zero (compare with results in next section), implying that the time average over a particle trajectory is equal to an ensemble average over all particles after a short time interval. It is worth noting that the number of particles does not affect the time for ergodicity.

For the sojourn times method, we considered two different cell sizes, $\Delta p = 0.5$ and two infinite cells: $p > 0$ and $p < 0$. The histograms (distribution functions) of sojourn times

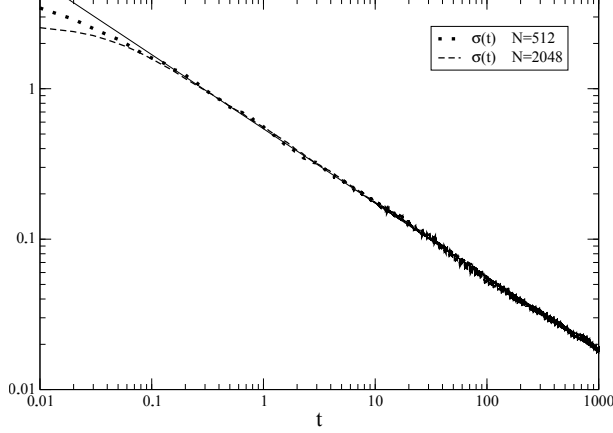


FIG. 1. Standard deviation in Eq. (6) of the variables \bar{p}_k with $N = 512$ and $N = 2048$ for the Hamiltonian in Eq. (3). The thin continuous line gives the best least-squares fit for the power law part of the plot and is given by $\sigma(t) = 0.542 \times t^{-0.493}$. The softening parameter was set to $\epsilon = 10^{-3}$.

are shown in Fig. 2 for $N = 512$ and $N = 2048$. In all cases a distinctive exponential tail indicating that the system is ergodic (no power law in the tail).

Finally for the dynamical functional method, Fig. 3 shows the real and imaginary parts of $E(n)$ and $Q(n)$. The asymptotic values rapidly tend to zero in accordance with Eqs. (15) and (16) (up to some fluctuations in the mixing test), indicating that the system is not only ergodic but also mixing.

Having established a comparison standard with the short-range interacting case, We now look at the two-dimensional self-gravitating system in the next section.

IV. TWO-DIMENSIONAL GRAVITY

For the self-gravitating N -body system with Hamiltonian in Eq. (2), we consider an initial condition with all particles at rest and distributed in space uniformly on a circular strip with inner radius $R_1 = 40.0$ and outer radius $R_2 = 50.0$. The standard deviation of the time average of the momentum of each single particle as given in Eq. (6) is shown in Fig. 4a for a few value of N ranging from 64 to 16 384, while Fig. 4b shows the Kurtosis of the momentum distribution defined by $K = \langle p^4 \rangle / \langle p^2 \rangle^2$, showing that after the initial violent relaxation the system is indeed in a QSS. By a direct comparison with Fig. 1, we observe that the time for ergodicity is at least two orders of magnitude higher than for the short

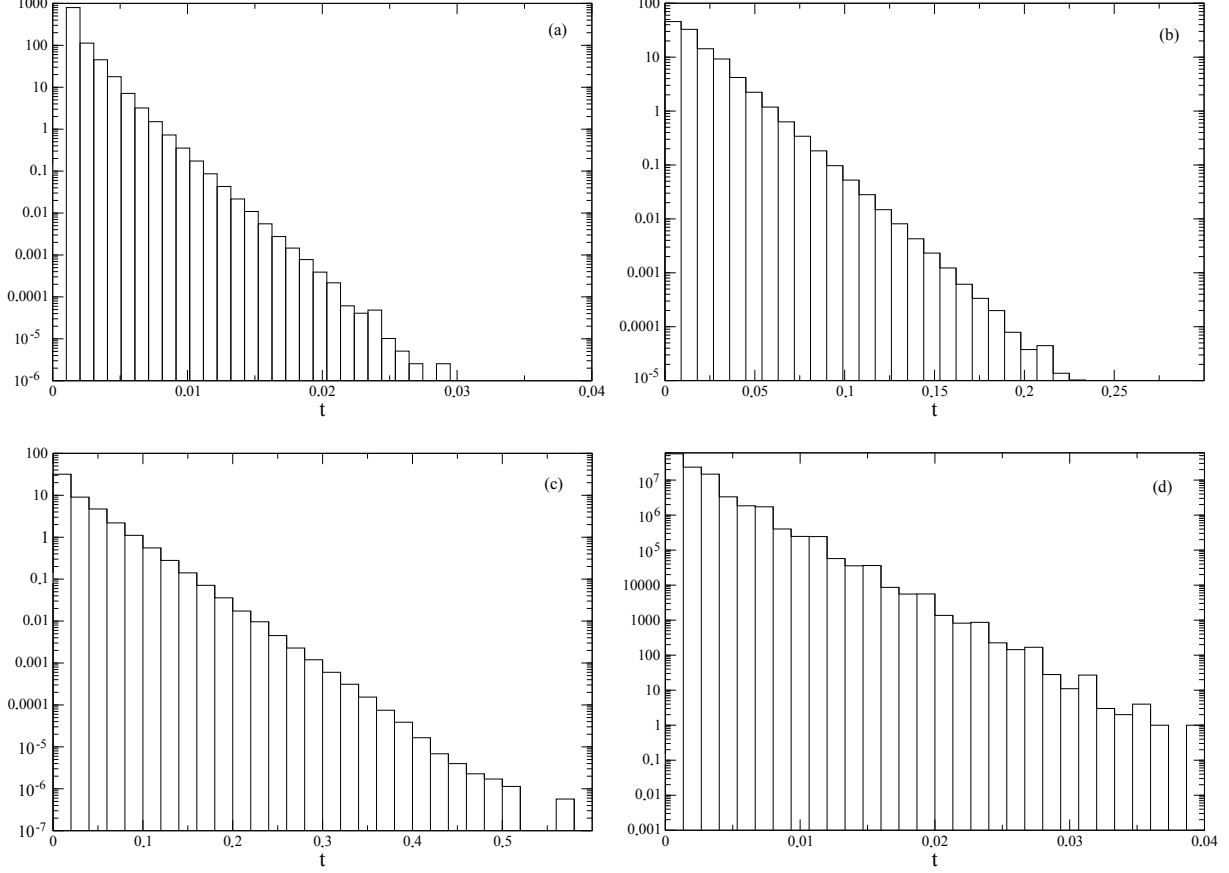


FIG. 2. a) Mono-Log plot of histogram of sojourn times with cells in momentum space of width $\Delta p = 0.5$ and $N = 512$ and total simulation time $t_f = 1000.0$. b) Same as (a) but with only two cells with $p > 0$ and $p < 0$. c) Same as (a) but with $N = 2048$ d) Same as (b) but with $N = 2048$ and $t_f = 100.0$. All histograms show clearly an exponential tail.

range case. More intriguingly is the fact that this characteristic time is the same for all values of N , as attested by the fact that the plots of $\sigma(t)$ collapse in the tail for all values of N . The exponent in the power law tails is close to -1 , indicating a strong auto-correlation in momentum.

Considering now the sojourn times statistics method, we divide momentum space into equal size cells of fixed width associated with discrete states. First we consider cells of width $\Delta p = 0.2$ for particle numbers $N = 2048$ and 8192 . Figure 5 shows the normalized histograms for sojourn times. We first note that even for a very large simulation time $t_f = 10^6$ the distribution of sojourn times is truncated at quite a small value. This truncation is expected to occur for finite systems as discussed at length for the Hamiltonian mean field

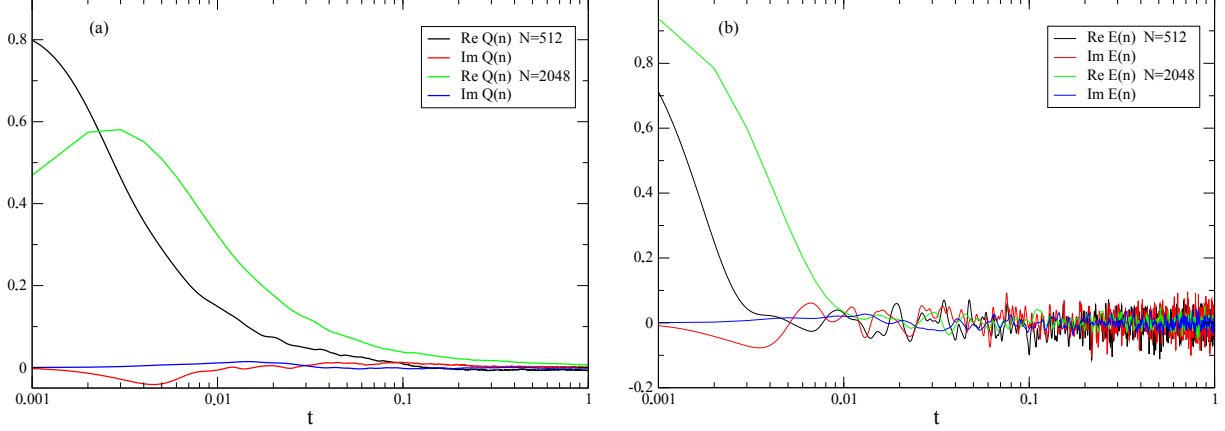


FIG. 3. (Color online) Left panel: Real and imaginary part of $Q(n)$ from Eq. (15) for the Hamiltonian in Eq. (3) with $\alpha = 3$, $N = 512$ and integration time step $\Delta t = 10^{-6}$. Note that $n = t/\Delta t$. Right panel: Evolution of $E(n)$ in Eq. (16) with time.

model in Ref. [15]. On the other hand the truncation values does not vary significantly with N , at variance with what was observed in Ref. [15]. One cannot ascribe a power law to the final part of the tail just before the truncation. Much longer simulation times would be required to obtain a better statistics for the tail, which is unfeasible in practice. This problem can be overcome by considering just two cells for $p < 0$ and $p > 0$ as shown in Fig. 6, where a power law behavior is visible at the end of the tail. In fact we observe two distinctive regimes in the tail, each satisfying a power law relation.

For the dynamical functional method initial conditions are the same as above. Figures 7 and 8 show the evolution with time of $Q(n)$ and $E(n)$, with $n = t/\Delta t$, as defined in Eq. (14) for a few values of N . In all cases Eqs. (15) and (16) are satisfied only after a very long time (compare with Fig. 3) which is roughly the same for all values of N , in agreement with our results above. Figure 9 shows the Kurtosis of the momentum distribution for $N = 128$ and $N = 8192$, ensuring that the state is very close to stationary, as required for the present method.

In order to verify if this N independence of the time for ergodicity is not related to the initial conditions with all particles at rest, we performed a simulation with the same initial spatial distribution, but with particle momenta uniformly distributed in an interval $-p_0/2 \leq p \leq p_0/2$, with $p_0 = 1.0$. Figure 10 shows the plot of $\sigma(t)$ for $N = 1024$ and $N = 4096$ and both closely coincide after the violent relaxation.

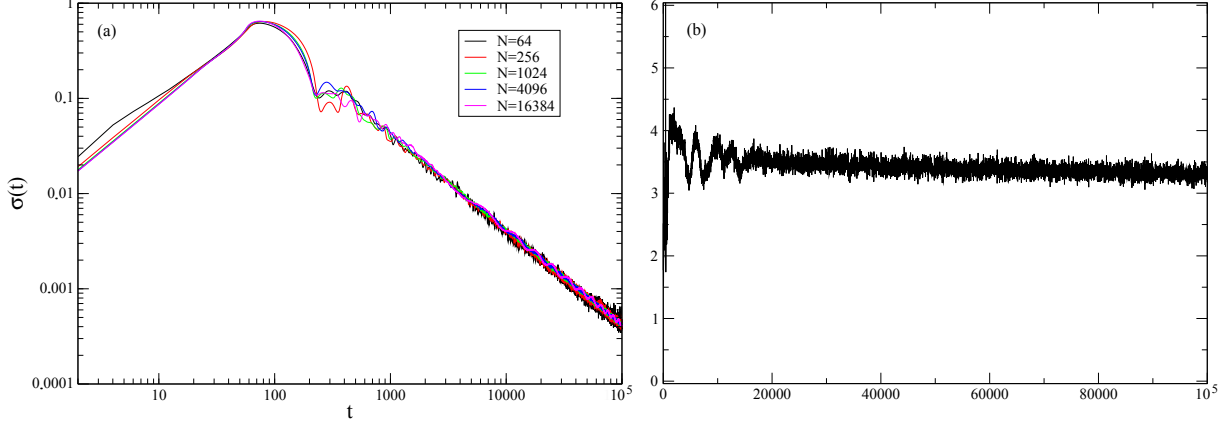


FIG. 4. (color online) Left panel: Standard deviation in Eq. (6) of the variables \bar{p}_k for the Hamiltonian in Eq. (2). The initial condition is a spatially uniform distribution on a circular strip with inner radius $R_1 = 40.0$ and outer radius $R_2 = 50.0$ and integration time step $\Delta t = 0.05$. The least-squares fit for the algebraic tail (not shown) is given by $\sigma(t) = 48.4 \times t^{-1.02}$. Right panel: Kurtosis of the momentum distribution as a function of time for $N = 4096$. The initial violent relaxation is visible and afterward the system settles in a QSS.

V. CONCLUDING REMARKS

We applied three different testes for ergodicity and on for mixing, presented in Section II for two systems: a short-range and a long-range interacting two-dimensional self-gravitating system. For the former all three methods point conclusively that the system is ergodic and that the time to attain ergodicity, is much smaller than for the two-dimensional self-gravitating long-range interacting system. The applications of the same methods for the latter showed that this time is at least two orders of magnitude larger than for the short-range case. While the direct and dynamical functional methods proved to be precise for testing ergodicity for self-gravitating system, the sojourn times gave more ambiguous results, as the possibly algebraic tail is too short in the present case. This is in contrast with results for the HMF model in Ref. [15] obtained for a homogeneous state (zero mean-field), that imply much longer sojourn times, while for a non-vanishing mean-field as in the present case, sojourn times are too small in order to precisely determine the tail of their distribution.

An important and unexpected result of the present work is the apparent independence on N of the time for ergodicity for the self-gravitating system. We note that up to the

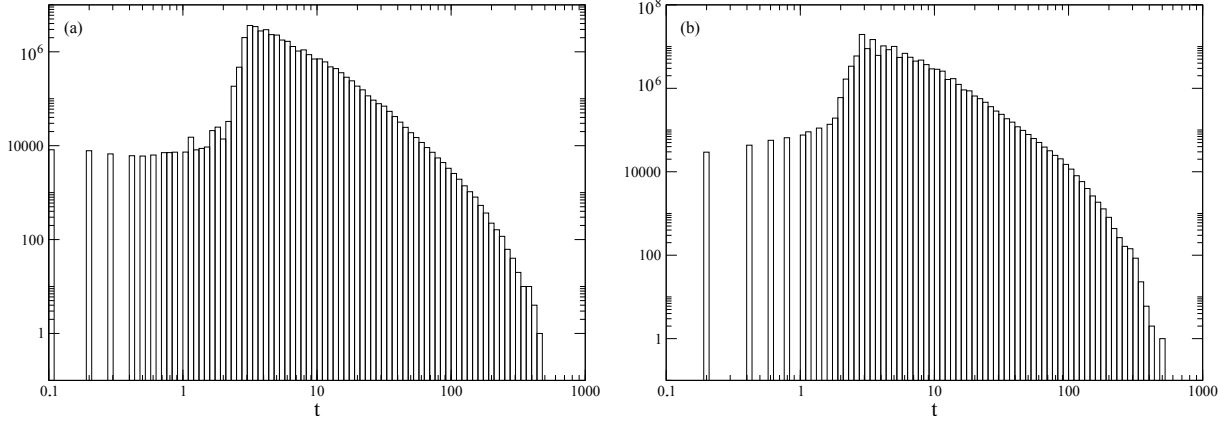


FIG. 5. a) Sojourn times for cells of width $\Delta p = 0.2$, for a circular strip initial condition in position with inner radius $R_1 = 40.0$ and outer radius $R_2 = 50.0$ and all particles at rest, $N = 2048$, total simulation time $t_f = 10^5$, and softening parameter $\epsilon = 10^{-3}$. b) Same as (a) but with $N = 8192$.

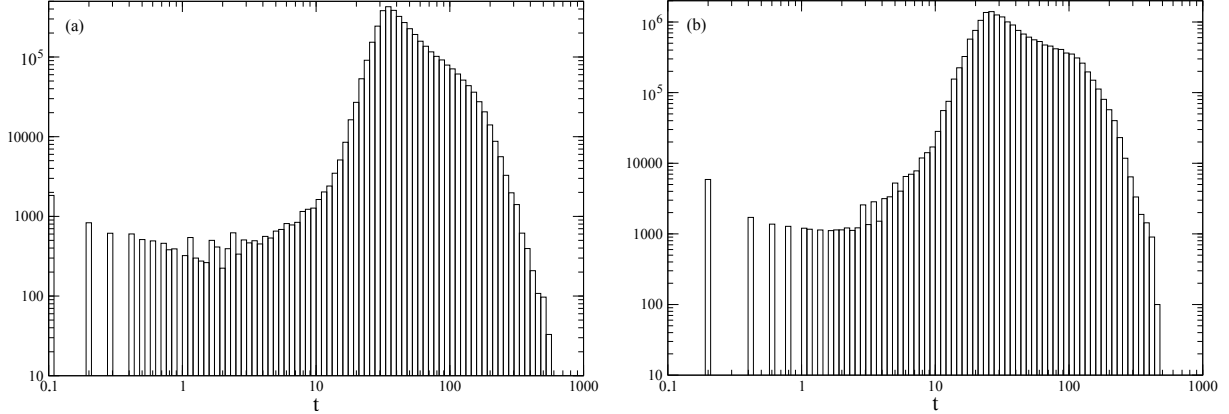


FIG. 6. Same as Fig. 5 but with two cells defined by $p < 0$ and $p > 0$.

authors knowledge the only previous works where such characteristic time was estimated for long-range interacting systems were devoted to the Hamiltonian mean field model, where a N dependence was reported [9, 15]. The collisional dynamics of the two-dimensional self-gravitating system scales with N as the collisional integral in the Balescu-Lenard kinetic equation, which is the proper equation in the present case, is of order N^{-1} [33], while the standard deviation $\sigma(t)$ does not depend on N . This apparent contradiction will be the subject of further investigations on the present model as well for other model systems with

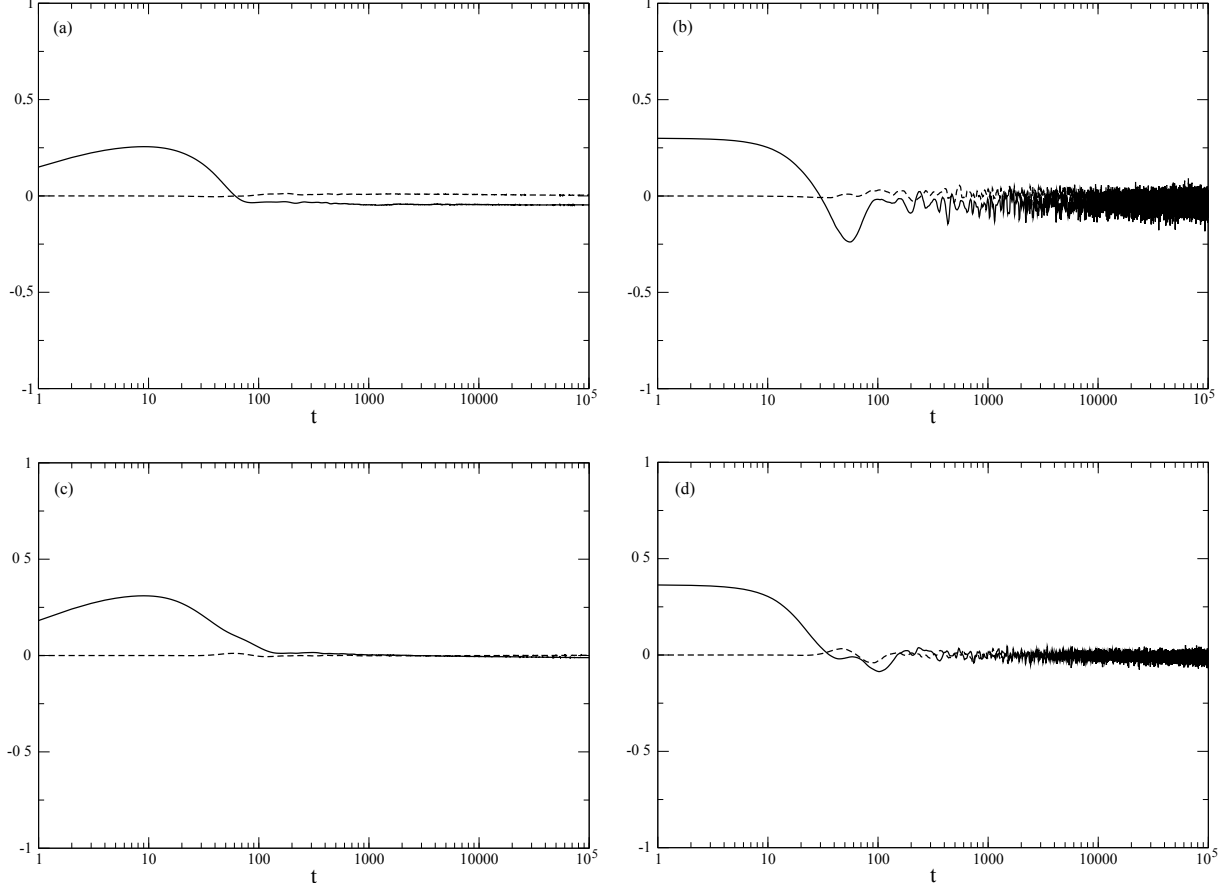


FIG. 7. a) Real (continuous line) and imaginary (dashed line) part of $Q(n)$ in Eq. (15) for the a two-dimensional self-gravitating system with Hamiltonian in Eq. (2), $N = 128$, integration time step $\Delta t = 0.1$ and $n = t/\Delta t$. b) Evolution of $E(n)$ in Eq. (16) with time, the simulations parameters as in (a). c) same as (a) but with $N = 512$. d) same as (b) but with $N = 512$.

long-range interactions.

-
- [1] A. Campa, T. Dauxois, D. Fanelli and S. Ruffo, *Physics of Long-Range Interacting Systems*, (Oxford Univ. Press, Oxford, 2014).
 - [2] *Dynamics and Thermodynamics of Systems with Long-Range Interactions*, T. Dauxois, S. Ruffo, E. Arimondo and M. Wilkens Eds. (Springer, Berlin, 2002).
 - [3] *Dynamics and Thermodynamics of Systems with Long-Range Interactions: Theory and Experiments*, A. Campa, A. Giansanti, G. Morigi and F. S. Labini (Eds.), AIP Conf. Proceedings

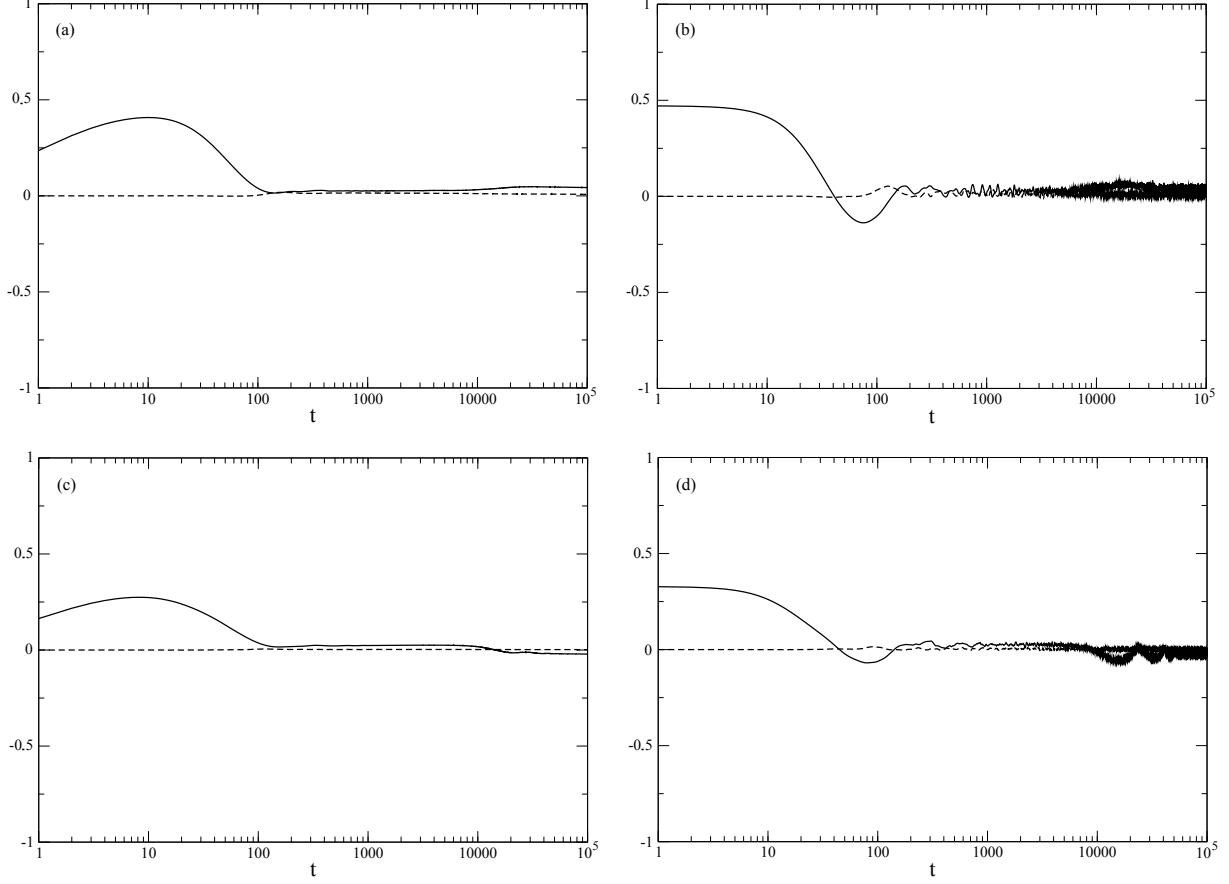


FIG. 8. Same as in Fig. 7 but with (a) and (b) with $N = 2048$ and (c) and (d) with $N = 8192$.

Vol. 970 (2008).

- [4] *Long-Range Interacting Systems, Les Houches 2008, Session XC*, T. Dauxois, S. Ruffo and L. F. Cugliandolo Eds. (Oxford Univ. Press, Oxford, 2010).
- [5] A. Campa, T. Dauxois and S. Ruffo, Phys. Rep. **480**, 57 (2009).
- [6] D. Lynden-Bell, Mon. Not. R. Astr. Soc. **136**, 101 (1967).
- [7] M. Antoni and S. Ruffo, Phys. Rev. E **52**, 2361 (1995).
- [8] D. Mukamel, S. Ruffo and N. Schreiber, Phys. Rev. Lett. **95**, 240604 (2005).
- [9] A. Figueiredo, T. M. Rocha Filho and M. A. Amato, Eur. Phys. Lett **83**, 30011 (2008).
- [10] F. Bouchet, T. Dauxois, D. Mukamel and S. Ruffo, Phys. Rev. E **77**, 011125 (2008).
- [11] P. H. Chavanis, Eur. Phys. J. B **80**, 275 (2011).
- [12] F. P da C. Benetti, T. N. Teles, R. Pakter and Y. Levin, Phys. Rev. Lett. **108**, 140601 (2012).
- [13] R. Pakter and Y. Levin, J. Stat. Phys. **150**, 531 (2013).

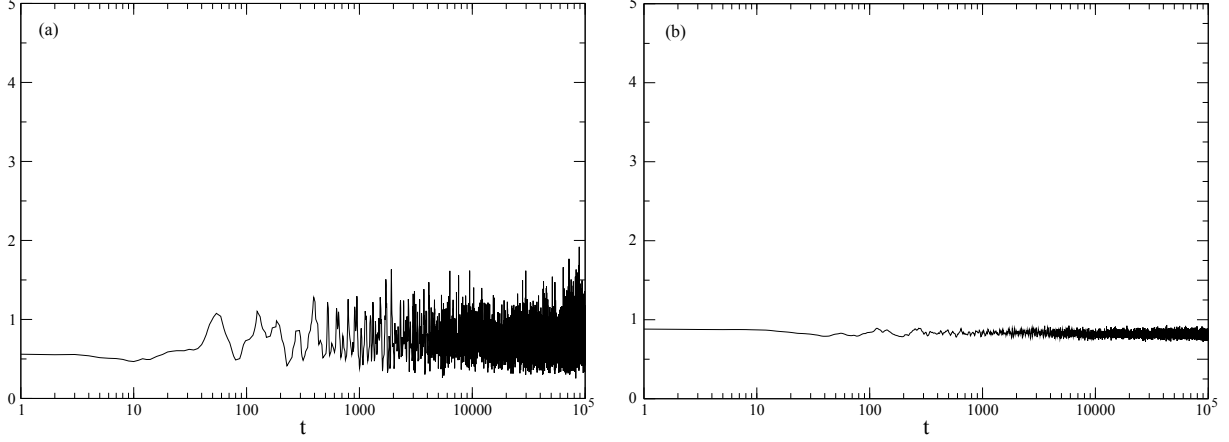


FIG. 9. Kurtosis for the momentum distribution as a function of time for (a) $N = 128$ and (b) for $N = 8192$. The is in a stationary state.

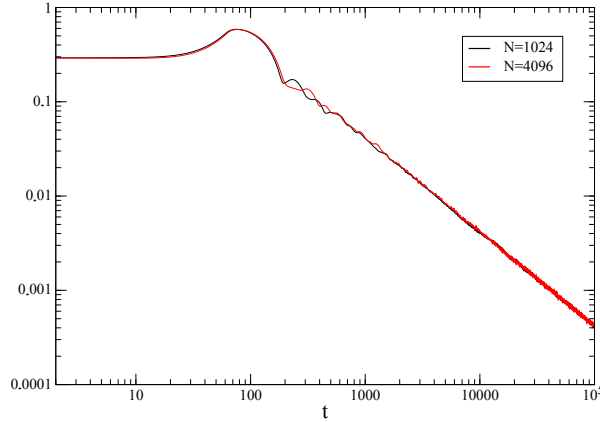


FIG. 10. (Color online) Standard deviation $\sigma(t)$ for the time averages of each particle momentum for the same spatial initial distribution as in Fig. 4a but for a uniform distribution for momenta in the interval $0.5 \leq p \leq 0.5$, for $N = 1024$ and $N = 4096$. The time for ergodicity is also the same.

- [14] A. C. Ribeiro-Teixeira, F. P. C. Benetti, R. Pakter and Y. Levin, Phys. Rev. E **89**, 022130 (2014).
- [15] A. Figueiredo, T. M. Rocha Filho, M. A. Amato, Z. T. Oliveira, Jr. and R. Matsushita, Phys. Rev. E **89**, 022106 (2014).
- [16] K. R. Yawn and B. N. Miller, Phys. Rev. E **56**, 2429 (1997).
- [17] K. R. Yawn and B. N. Miller, Phys. Rev. E **68**, 056120 (2003).
- [18] P. Heand D.-B. Kang, Mon. Not. R. Astron. Soc. **406**, 2678 (2010).

- [19] J. C. Maxwell, *On Boltzmann's Theorem on the average distribution of energy in a system with material points*, Cambridge Philosophical Society's Transactions, (London, 1876).
- [20] G. D. Birkhoff, Proc. Nat. Aacas. Sci. **17**, 656 (1931).
- [21] A. I. Khinchin, *Mathematical Foundations of Statistical Mechanics*, Dover (New York, 1957).
- [22] A. Rebenshtok and E. Barkai, J. Stat. Phys. **133**, 565 (2008).
- [23] A. Saa and R. Venegeroles, Phys. Rev. E **82**, 031110 (2010).
- [24] T. Tsuchiya, T. Konishi and N. Gouda, Phys. Rev. E **50**, 2607 (1994).
- [25] A. Janicki and A. Weron, *Simulation and Chaotic Behaviour of α -Stable Stochastic Processes*, Marcel Dekker, (New York, 1994).
- [26] S. Cambanis, K. Podgorski and A. Weron, Studia Math. **115**, 109 (1995).
- [27] M. Magdziarz and A. Weron, Phys. Rev. E **84**, 051138 (2011).
- [28] T. M. Rocha Filho, Comp. Phys. Comm. **185**, 1364 (2014).
- [29] Y. Levin, R. Pakter, F. B. Rizzato, T. N. Teles and F. P. C. Benetti, Phys. Rep. **535**, 1 (2014).
- [30] M. Antoni and A. Torcini, Phys. Rev. E **57**, R6233 (1998).
- [31] J. J. Aly and J. Perez, Phys. Rev. E **60**, 5185 (1999).
- [32] B. Marcos, Phys. Rev. E **88**, 032112 (2013).
- [33] T. M. Rocha Filho, M. A. Amato, A. E. Santana, A. Figueiredo and J. R. Steiner, Phys. Rev. E **89**, 032116 (2014).
- [34] T. N. Teles, Y. Levin, R. Pakter and F. B. Rizzato, J. Stat. Mech. P05007 (2010).
- [35] K. Faghei and M. Pak, Astrophys Space Sci. **353**, 641(2014).
- [36] S. J. Aarseth, *Gravitational N-Body simulations*, Cambridge Univ. Press (Cambridge, 2003).
- [37] T. M. Rocha Filho, *Non-equilibrium Entropy and Dynamics in a System with Long-Range Interactions*, [cond.mat:stat-mech].